Jurnal Teknologi

Full Paper

THE OPTIMIZATION OF PASSIVE MICROMIXERS WITH THREE-SPLIT RHOMBIC SUB-CHANNELS FOR CHEMICAL ANALYSIS APPLICATION

Roer Eka Pawinanto[a*], Erni Nuraini[b], Budi Mulyanti[a], Ahmad Aminudin[b], Devi Fitria Nurvadila[b], Chandra Wulandari[b,c], Jumril Yunas[d], Lilik Hasanah[b]

[a]Departement of Electrical Engineering Education, Universitas Pendidikan Indonesia, Bandung 40154, Jawa Barat, Indonesia
[b]Departement of Physics Education, Universitas Pendidikan Indonesia, Bandung 40154, Jawa Barat, Indonesia
[c]Engineering Physics, Institut Teknologi Bandung, Bandung 40132, Jawa Barat, Indonesia
[d]Institute of Microengineering and Nanoelectronics (IMEN), Universiti Kebangsaan Malaysia (UKM), Bangi 43600, Selangor, Malaysia

Article history
Received
16 November 2021
Received in revised form
15 June 2022
Accepted
25 July 2022
Published Online
31 October 2022

*Corresponding author
roer_eka@upi.edu

Graphical abstract

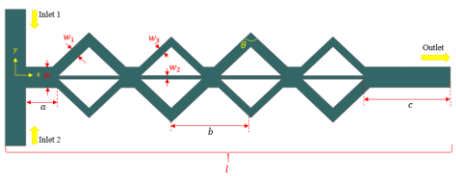

Abstract

A rhombic with unbalanced three-split in a passive micromixer is studied. This work aims to optimize micromixers' three-split rhombic design for chemical analysis through mixing index and pressure drop analysis. The optimization was obtained by varying the angle of the rhombic and the ratio of the sub-channel widths, including angles of 30°, 45°, 60°, 90° and widths of 150:100 µm, 200:100 µm, 250:100 µm, and 300:100 µm. The COMSOL Multiphysics was used to simulate the performance based on a three-dimensional Navier-Stokes equation with the working fluid model in the form of water in the advection-diffusion model. A parametric study was carried out to evaluate the effect of the geometric micromixer variable on the mixing performance for the Reynolds range of 10-120. The results show that a micromixer with an unbalanced triangular rhombic the structure with an angle of 30° and width of 200:100 µm on Re 120 achieve mixing efficiency at 0.91 with pressure drop 1700 Pa.

Keywords: Micromixer, three-split rhombic, Reynolds number, Mixing Index, Navier-Stokes Equation

Abstrak

Satu rombus dengan tiga pecahan tidak seimbang dalam pengadun mikro pasif telah dikaji. Kerja ini bertujuan untuk mengoptimumkan pengadun mikro dengan reka bentuk tiga bahagian rombus untuk analisis kimia melalui indeks pencampuran dan analisis penurunan tekanan. Pengoptimuman diperoleh dengan mengubah sudut rombus dan nisbah lebar sub saluran, meliputi sudut 30°, 45°, 60°, 90° dan lebar 150:100 m, 200:100 m, 250: 100 m, dan 300:100 m. COMSOL Multiphysics digunakan untuk mensimulasikan prestasi berdasarkan persamaan Navier-Stokes tiga dimensi dengan model bendalir kerja dalam bentuk air dalam model adveksi-resapan. Kajian parametrik telah dijalankan untuk menilai kesan pembolehubah mikropembolehubah geometri ke atas

prestasi pencampuran bagi julat Reynolds 10-120. Keputusan menunjukkan bahawa pengadun mikro dengan rhombik segi tiga tidak seimbang struktur dengan sudut 30° dan lebar 200:100 µm pada Re 120 mencapai kecekapan pencampuran pada 0.91 dengan penurunan tekanan 1700 Pa.

Kata kunci: Micromixer, rombus dengan tiga pecahan, nombor Reynolds, indeks campuran, formula Navier Stokes

© 2022 Penerbit UTM Press. All rights reserved

1.0 INTRODUCTION

Lab on Chip (LoC) is a research topic that is widely used in various disciplines, including chemical reactions [1], chemical synthesis [2, 3], chemical analysis [4], etc. Advantages of LoC in combines [5], miniaturizes [6], and portable [7], make the topic continue to grow and increase rapidly in instrumentation or industry [5]. The microfluidic device is one part of the LoC that handles the control and manipulation of fluids on a small-scale geometry [8]. The small fluidity (laminar flow) makes mixing difficult in microsystems [9, 10, 11]. On a microscale, the mixing occurs as a result of the molecular diffusion process. Therefore, a micromixer design to enhance the mixing process is required. [12, 13, 14, 15].

Generally, Micromixer can be categorized into two groups, namely active and passive micromixers [9]. Active micromixers require some external energy source or moving parts to stimulate flow. In addition, they are generally more efficient at mixing than passive micromixers. However, the drawback is difficult to manufacture and integrate with major microfluidic systems [10, 11]. In contrast, passive micromixers do not require external energy to separate and mix the streams [16].

Furthermore, passive micromixers are easy to manufacture and do not require external power or force to manipulate the fluid [13]. Passive micromixers do not always require a low Re or a fixed flow rate for their operation. Consequently, passive micromixers are used in most microfluidic applications rather than active micromixers [16]. The passive micromixer utilizes the flow rate energy (provided by the pump, the static pressure difference, and the geometry of the micromixer) to separate and mix the flow [14]. The separation and mixing of streams can enhance the diffusion process and promote a convection-based secondary flow [17].

Previous studies have developed many structures of micromixer passive based on lamination [18], obstacles [19], divergence-convergence [5], and asymmetrical structures [20]. However, in convergence-divergence based on micromixer, the mixing quality improves as the convergence-divergence configuration is usually combined with other patterns such as resistance-based, Split, and Recombined (SAR) [5]. Fang and Yang (2009) demonstrated that mixing using the SAR structure could create chaotic advection and showed better mixing performance at relatively high Reynolds numbers [21]. Schonfeld *et al.*, (2004) Conducted a numerical investigation of the SAR micromixer at various Reynolds (Re) numbers, mixing on the SAR mixer resulted in efficient mixing [22].

Based on previous studies, it can be concluded that the SAR micromixer effectively improves the mixing of liquids [5]. Chung and Shih (2007) revealed that combination effects of focusing/diverging, recirculation and Dean vortices lead to very high mixing efficiency [23]. The structure was developed by Schönfeld *et al.* [24]. They set the halves and triples rhombus and achieved a mixing efficiency of 86% for the triples at Re = 60. Bayareh *et al.* (2020) developed an unbalanced three-split rhombic sub-channel [17]. The three-dimensional Navier-Stokes equation combined with the advection-diffusion model using two types of fluids (water and ethanol). Mixing index and pressure drop were evaluated and compared with a two-split micromixer for the Reynolds number range from 0.1–120. The results showed that the proposed three-split micromixer is more efficient in mixing the Reynolds number range from 30–80 [17]. Parametric studies were carried out to determine the effect of rhombic angle and sub-channel width ratio on mixing and pressure drop. Although it is operating at the lowest Reynolds number, the rhombic angle of 90° provides the best mixing performance. The results show that the performance of a three-split micromixer with a minimum minor sub-channel width provides the best mixing performance [5, 9]. However, this study has a drawback where the pressure drop obtained is still relatively high. This pressure drop effect cannot be ignored because it can cause a cavitation effect for chemical analysis application, and the energy required to drain the liquid also increases.

In this paper, we investigate the three-split rhombic sub-channel micromixer by varying the angle of the rhombus and the ratio of the width of the sub-channel. This work was carried out at Re 10-120 using the COMSOL Multiphysics simulation, and the 3-D Navier-Stokes equation was used for mixing analysis using a working fluid in the form of water. Finally, this study is expected to produce a three-split rhombic design with mixing index >0.8 and pressure drop <3630 Pa.

2.0 METHODOLOGY

The schematic diagram of the SAR-based unbalanced three-section rhombic passive micromixer is shown in

Figure 1. Where the fluid is water with a density of 1025 $kg \cdot m^{-3}$ and dynamic viscosity 1.5×10^{-3} $kg \cdot m^{-1} \cdot s^{-1}$ enter through the inlet 1 and inlet 2 channels and then come into contact at the T channel junction. Mixing increases as the liquid flows splits into 3 lanes with varying angles and widths, then meet at the intersection. The division of the path is repeated several times so that the mixing index increases up to the outlet.

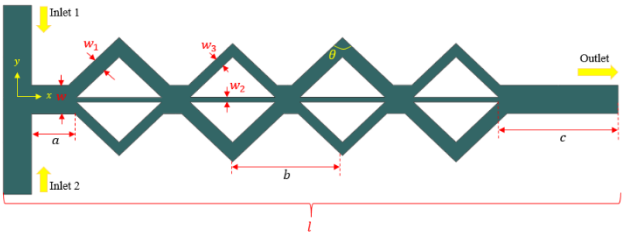

Figure 1 Schematic diagrams of rhombic micromixer unbalanced three-split rhombic micromixer

In this work, a parametric study was carried out to evaluate the effect of the geometric micromixer variable on the mixing performance for the Reynolds range of 10-120, which aims to obtain the most optimal geometry based on the mixing quality and to determine the effect of Reynolds number on mixing and pressure drop. In geometry (w_1) serves as the main sub-channel width, (w_2) serves as the minor sub-channel 1 width, and (θ) serves as the rhombic angle.

In this case, controlling the sub-channel width is done by changing the outer wall with a constant inner wall. Furthermore, for the number of rhombic units, inside rhombic height (h) and the channel width when making angle θ changes must be kept constant.

Dimensions based on the designed geometric structure are shown in Table 1 as shown in Table 1, the total length used is 6.5 mm with an inlet length of 1000 μm. The parameter study on the width (w_1: w_3) with each value are 150:100 μm, 200:100 μm, 250:100 μm, and 300:100 μm, as well as the variation of the angle with the value of 30°, 45°, 60°, 90°.

Table 1 The design dimension of the microfluidic mixer

No.	Parameters	Values
1	Length (l)	6.5 mm
2	Width (w)	300 µm
3	$w_1 : w_2$	150:100,200:100,250:100,300:100
4	w_2	50 µm
5	Inlet length	1000 µm
6	Inlet width	500 µm
7	Angle (θ)	30°, 45°, 60°, 90°
8	a	475 µm
9	b	1.2 mm
10	c	3 mm

Numerical studies are used for simulation modelling on software COMSOL Multiphysics. Module Navier-Stokes Incompressible and module Convection Diffusion is selected in this device. The properties of the liquids are shown in Table 2. Moreover, the mesh setting coarse in COMSOL is used due to the limitation of time calculation and computer performances. It provides around 158,587 of total domain elements calculate during the computation.

Table 2 Property of fluid

Fluid	Density($kg \cdot m^{-3}$)	Dynamic viscosity ($kg \cdot m^{-1} \cdot s^{-1}$)
water	1025	1.5×10^{-3}

The primary and secondary fluids each use a solution with a different concentration. The concentration used is C_1 = 1 mol/L and C_2 = 5 mol/L. To determine the fluid velocity associated with the Re number, the hydraulic diameter (D_h) is determined using equation (1).

$$D_h = \frac{2(ab)}{a+b} \tag{1}$$

Where *a* is the width of the geometry and *b* is the length of the geometric plane. Meanwhile, the flow velocity (*u*) from the inlet is determined by equation (2).

$$u = Re\frac{\mu}{\rho D_h} \tag{2}$$

Where *Re* is the Reynolds number, μ is the dynamic viscosity, ρ is the density and (D_h) is the hydraulic diameter. Based on equation (2), Re affects the flow velocity. The greater the number Re specified, the greater the flow velocity. The equations used are the Navier Stokes equation, the continuity equation, and the diffusion-convection equation which are generally described using equations (3) - (5).

$$\rho\left[\frac{\partial u}{\partial t} + (u.\nabla)u\right] = -\nabla p + \mu\nabla^2 u \tag{3}$$

$$\nabla u = 0 \tag{4}$$

$$\frac{\partial c}{\partial t} = D\nabla^2 - u.\nabla C \tag{5}$$

Where u denotes velocity, *ρ* is the density of the fluid, *p* is the pressure, and *μ* is the dynamic viscosity of the fluid. *C* and *D* represent concentration and diffusion, respectively.

The output performance to be obtained from this study is mixing index (*M*). This performance can be calculated using the standard deviation of mass fraction for each sampling point in the cross-section, as seen in equations (6) and (7).

$$\sigma = \sqrt{\frac{1}{n}\sum_{i=1}^{n}(Ci - Cs)^2} \tag{6}$$

$$M = 1 - \sqrt{\frac{\sigma^2}{\sigma_{max}^2}} \tag{7}$$

Where *n* is the sampling points inside cross-section, C_i is the mass fraction at the sampling point *i*, and C_s is the mean of the mass fraction, σ is the concentration at *a*

certain cross-sectional area of the microfluidic mixer, σ_{max} is the standard deviation at the inlets. The value of mixing index is evaluated in the range of 0 to 1, where a value of 0 indicates that the solution has not been mixed completely, whereas a value of 1 show that the solution is perfectly mixed.

3.0 RESULTS AND DISCUSSION

3.1 Comparison between Three-Split Micromixers Variation of width

The performance of an unbalanced three-split rhombic micromixer width variation was evaluated. Based on the evaluation results, the mixing index value with a width ratio of 200:100 *μm* has been tested better. To analyze mixing, each mass fraction distribution of water is plotted at the exit of each rhombic unit. The mixing enhancement occurs when the circulation flows through the channel and induces secondary circulation. There are two small recirculating streams near the small sub-channel inlet that can provide the mixing improvement.

Figure 2 shows the variation of the mixing index for the variation of the width through the outlet of the rhombic unit (*l* = 6.5 *μm*) of the micromixer for the Reynolds number from 10-120 for the unbalanced three-split rhombic micromixer with the same axial length. For low Reynolds number (<1), molecular diffusion has an essential role in mixing. For low Reynolds number, mixing is affected by residence time and flow path length. As the Reynolds number increases, the value of the mixing index will decrease because it is affected by the decrease in residence time and reaches a minimum value at Re = 10. The unbalanced three-split rhombic micromixer showed the best mixing performance in the medium Reynolds number range (<120) based on the evaluation results. Figure 2 variations of width in the mixing index at the exit of the micromixer vs Reynolds number.

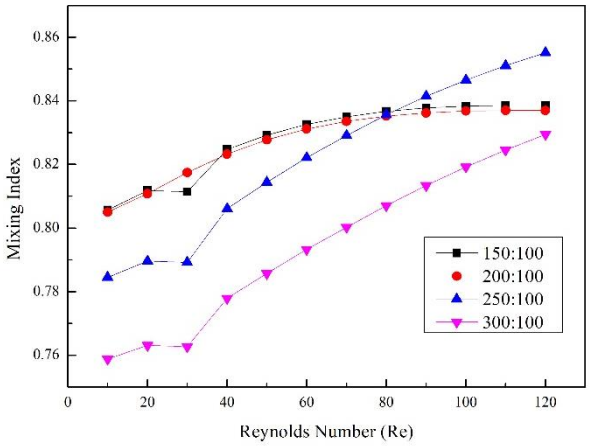

Figure 2 Variations of width in the mixing at the exit of the micromixer vs Reynolds number

Figure 3 shows the characteristic of the pressure drop as a function of the Reynolds number in the range Re 10-120 for variations in width and variation in angle. The pressure drop is calculated when the rhombic unit exits (l=6.5 μm). For low Reynolds number (<10), small wall friction and passive transverse flow occur. Beside the Re number 10, the unbalanced three-split rhombic micromixer provides a more significant pressure drop due to greater wall friction and higher transverse motion.

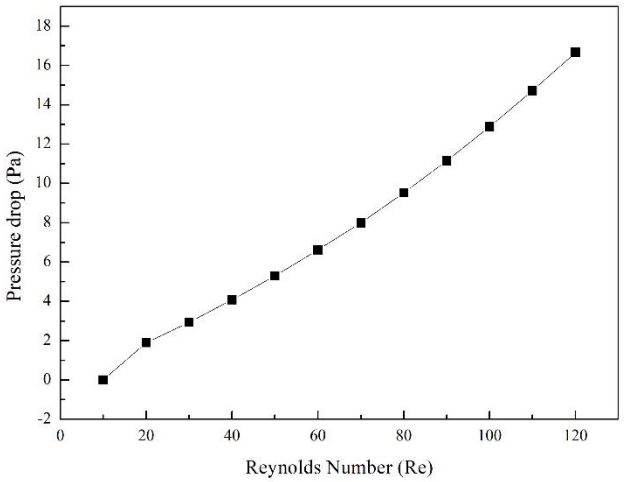

Figure 3 Variations of the pressure drop with Reynold number in unbalanced three-split rhombic micromixers

3.2 Comparison between Three-Split Micromixers Variation of Angle

The variation of the mixing index with the variation of the angle through the outlet of the micromixer for the Reynolds number from 10-120 for an unbalanced three-split rhombic micromixer with the same axial length is shown in Figure 4. Based on the evaluation results, the best mixing index value is at an angle of 30°. For low Re, the mixing index increases as the angle increases and the residence time also increases. Moreover, for low Re, the main mixing is regulated by molecular diffusion. Figure 4 shows the greatest variation in the mixing index is at the Re number 60 and the maximum mixing index is at an angle of 30°. For the case of the three-split micromixer shown as the angle increases, the total flow path increases as pitch increases with a fixed height.

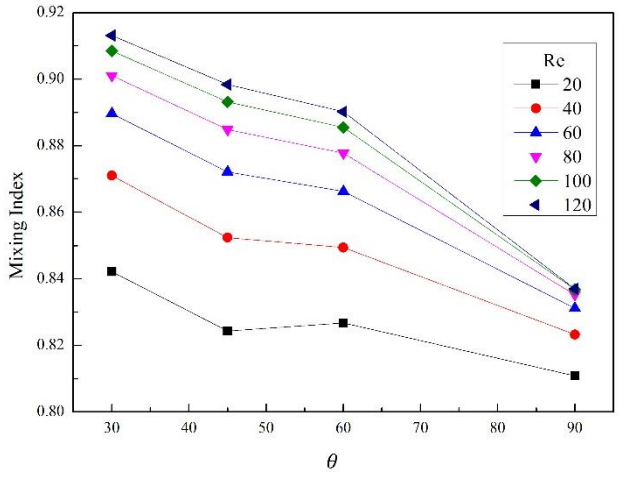

Figure 4 Effect of rhombic angle on mixing in the three-split micromixer vs Reynolds number

Figure 5 visualizes the effect of the angle of a rhombic on the pressure drop on an unbalanced three-split rhombic micromixer at Reynolds numbers 20, 40, 60, 80, 100, 120. The pressure drop will gradually increase when the speed is almost constant, i.e., when the angle reaches 30°-120°. For the case of the unbalanced three-split rhombic micromixer shown, as the angle increases, the total flow path increases due to the increase in pitch with a constant height effect on the pressure change.

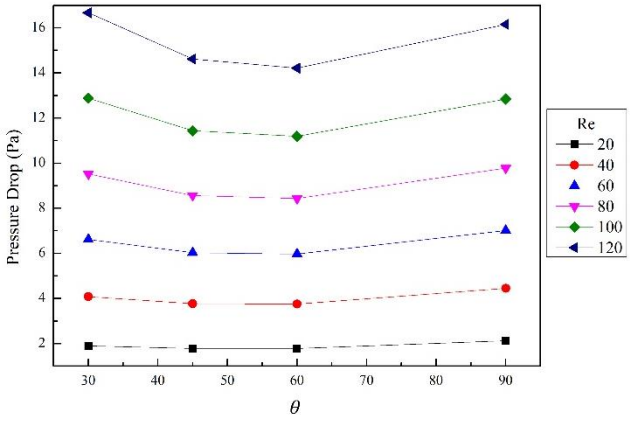

Figure 5 Effect of rhombic angle on the pressure drop in the three-split micromixer for vs Reynolds number

Figure 6 visualizes the velocity in a micromixer with a width of 200:100 µm and an angle of 30° on the Re 120. In this geometry, it is clear that along the microchannel, the fluid velocity is similar. Based on the results of the analysis, maximum velocity occurs when approaching the value of 0.8 m/s and as it approaches the microchannel wall it drops to 0. It occurs because the fluid layer's frictional force in the middle is much smaller than the frictional force around the walls. As a result, the velocity may decrease so that the minimum velocity is near the wall and the maximum velocity is at the center.

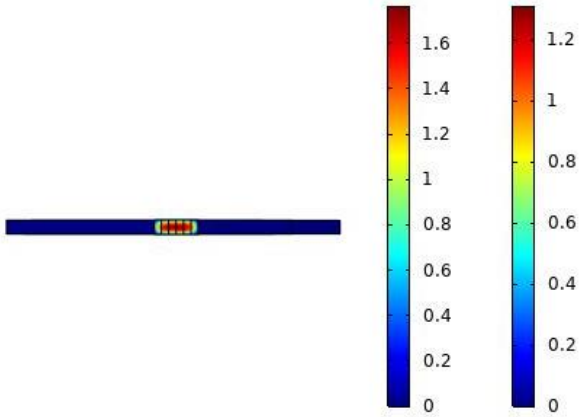

Figure 6 The fluid velocity of micromixer a width 200:100 µm with an angle 30° on Re 120

Figure 7 visualizes the mixing index process using different angles. A liquid concentration of 1 mol/m^3 is marked in blue for the first fluid, and the red color indicates a liquid concentration of 5 mol/m^3 for the second fluid. The mixture is homogeneous when it reaches the midpoint of 3 mol/m^3. The angle is varied to see the effect of mixing efficiency on the change in angle, shown in Figures 7(a)-(d). The micromixer is efficient with a ratio of 200:100 µm at an angle of 30°. As the fluid flows through the corners of the first rhombus structure, the cross section is distorted by the centrifugal force. centrifugal force pushes the liquid so that the liquid can rise to flow out of three zigzag channels, three streams are combined into one stream which can improve mixing. Therefore, this rhombic with unbalanced three-split in a passive micromixer structure can increase the residence time of the fluid in the channel, which can cause the fluid to be more chaotic so that the mixing process in the micromixer increases.

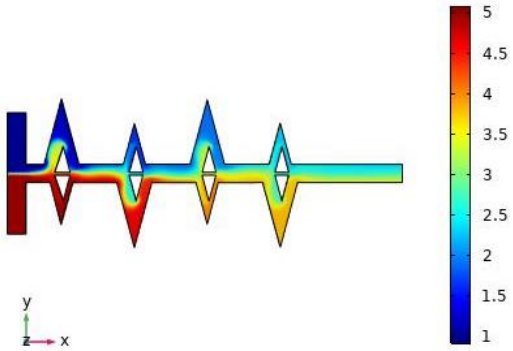

(a)

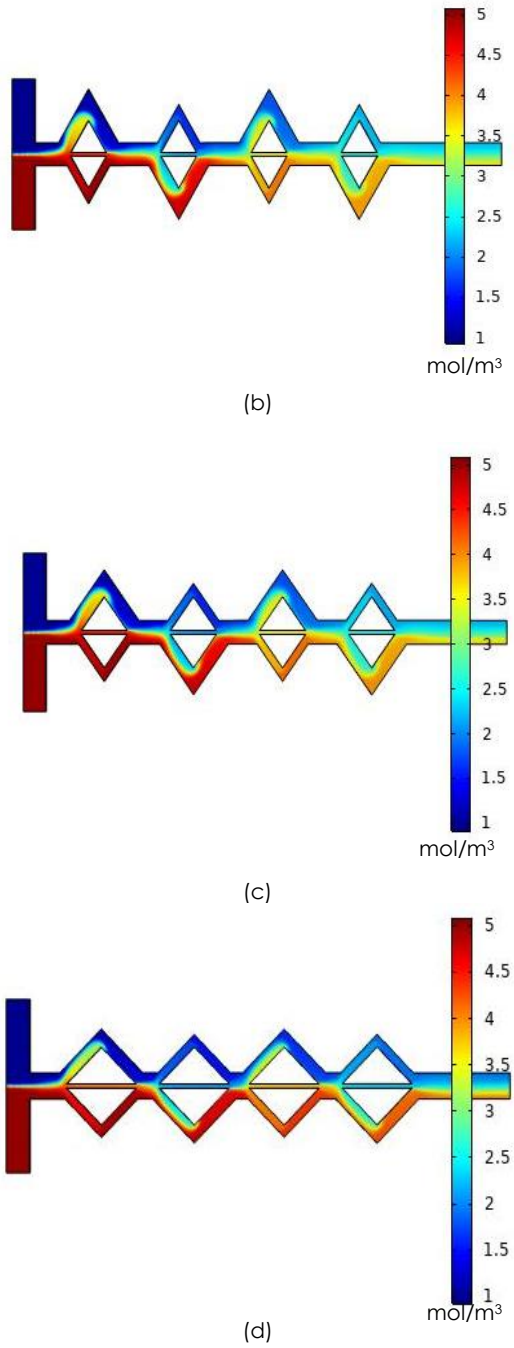

Figure 7 Concentration micromixer of ratio 200:100 µm (a) angle 30°, (b) angle 45°, (c) angle 60°, (d) angle 90°

Based on Table 3, it can be seen that this structure has an improvement from the previous article to contribute to the development of the micromixer. The design of the Three-split rhombic structure in this study resulted in better mixing efficiency with lower pressure drop values. Pressure drop occurs due to friction between fluids or through walls. This cannot be ignored because it can cause a cavitation effect, and the energy required for the liquid to flow also increases

Table 3 Comparison of our proposed micromixers with recent literature work

Structure	Mixing Index	Pressure Drop	Reference
Rhombic with assymetrical flow	0.84	3630 Pa	[20]
Three-split rhombic sub-channels	0.91	1700 Pa	Our research

4.0 CONCLUSION

A passive micro-mixer was designed WITH three-split rhombic sub-channels, uses COMSOL Multiphysics to show performance by using the three-dimensional Navier-Stokes equation in the advection-diffusion model with the water working fluid model. This research study determines the effect of micromixer geometric variables on mixing performance for chemical analysis in the Re 10-120. The result shows that the three unbalanced split rhombic structure produces a mixing index > 0.8 for each angle variation in various Re. As for the width variation, the mixing index obtained >0.8 in various widths except for the width of 250:100 µm with Re 10-30 and the width of 300:100 µm with Re 10-40. The effect of pressure drops for a constant angle at a width of 200:100 µm produces a pressure drop that increases with the increase in the Re number. It can be concluded, the structure with an angle of 30° and width of 200:100 µm on Re 120 achieve mixing efficiency at 0.91 with pressure drop 1700 Pa. This structure is compared with the existing structure in the literature resulting in better performance. It is expected that this design optimization applies to Lab on Chip such as chemical analysis applications.

Acknowledgments

The authors thank UPI for providing the facility for conducting progress meeting and IMEN, UKM to provide the software used in this study. This research was supported by funding from the Ministry of Education and Culture Indonesia with grant 275/UN40.LP/PT.01.03/2021 and Universitas Pendidikan Indonesia through World Class University (WCU) Program.

References

[1] Meller, K., Szumski, M., and Buszewski, B. 2017. Microfluidic Reactors with Immobilized Enzymes-Characterization, Dividing, Perspectives. *Sensors and Actuators B: Chemical*. 244: 84-106. DOI: https://doi.org/10.1016/j.snb.2016.12.021.

[2] Yang, A. S., Chuang, F. C., Chen, C. K., Lee, M. H., Chen, S. W., Su, T. L., and Yang, Y. C. 2015. A High-Performance Micromixer Using Three-Dimensional Tesla Structures for Bio-Applications. *Chemical Engineering Journal*. 263: 444-451. DOI: https://doi.org/10.1016/j.cej.2014.11.034.

[3] Wu, Y. T., Yang, C. E., Ko, C. H., Wang, Y. N., Liu, C. C., & Fu, L. M. 2020. Microfluidic Detection Platform with Integrated Micro-Spectrometer System. *Chemical Engineering Journal*. 393: 124700.
DOI: https://doi.org/10.1016/j.cej.2020.124700.

[4] Zhang, Y., G,e S. and Yu, J. 2016. Chemical and Biochemical Analysis on Lab-On-A-Chip Devices Fabricated Using Three-Dimensional Printing. *TrAC Trends in Analytical Chemistry*. 85: 166-180.
DOI: https://doi.org/10.1016/j.trac.2016.09.008.

[5] Hossain, S. and Kim, K. Y. 2014. Mixing Analysis of Passive Micromixer with Unbalanced Three-Split Rhombic Sub-Channels. *Micromachines*. 5(4): 913-928.
DOI: https://doi.org/10.3390/mi5040913.

[6] Raza, W. and Kim, K. Y. 2019. An Unbalanced Split and Recombine Micromixer with Three-Dimensional Steps. *Industrial & Engineering Chemistry Research*. 59(9): 3744-3756.
DOI: https://doi.org/10.1021/acs.iecr.9b00682.

[7] Mondal, B., Mehta, S. K., Patowari, P. K., and Pati, S. 2019. Numerical Study of Mixing in Wavy Micromixers: Comparison Between Raccoon and Serpentine Mixer. *Chemical Engineering and Processing-Process Intensification*. 136: 44-61.
DOI: https://doi.org/10.1016/j.cep.2018.12.011.

[8] Borgohain, P., Arumughan, J., Dalal, A., and Natarajan, G. 2018. Design and Performance of a Three-Dimensional Micromixer with Curved Ribs. *Chemical Engineering Research and Design*. 136: 761-775.
DOI: https://doi.org/10.1016/j.cherd.2018.06.027.

[9] Stone, H. A., Stroock, A. D., and Ajdari, A. 2004. Engineering Flows in Small Devices: Microfluidics Toward a Lab-On-A-Chip. *Annual Review Fluid Mechanics*. 36: 381-411.
DOI: https://doi.org/10.1146/annurev.fluid.36.050802.122124.

[10] Wang, H., Iovenitti, P., Harvey, E., & Masood, S. 2002. Optimizing Layout of Obstacles for Enhanced Mixing in Microchannels, Smart Materials and Structures. 11(5): 662.
DOI: https://doi.org/10.1088/0964-1726/11/5/306.

[11] Julius, L. A. N., Jagannadh, V. K., Michael, I. J., Srinivasan, R., and Gorthi, S. S. 2016. Design and Validation of On-Chip Planar Mixer Based on Advection and Viscoelastic Effects. *BioChip Journal*. 10(1): 16-24.
DOI: https://doi.org/10.1007/s13206-016-0103-1.

[12] Shi, H., Zhao, Y. and Liu, Z. 2020. Numerical Investigation of the Secondary Flow Effect of Lateral Structure of Micromixing Channel on Laminar Flow. *Sensors and Actuators B: Chemical*. 321: 128503.
DOI: https://doi.org/10.1016/j.snb.2020.128503.

[13] Jeon, W. and Shin, C. B. 2009. Design and Simulation of Passive Mixing in Microfluidic Systems with Geometric Variations. *Chemical Engineering Journal*. 152(2-3): 575-582.
DOI: https://doi.org/10.1016/j.cej.2009.05.035.

[14] Milotin, R. and Lelea, D. 2016. The Passive Mixing Phenomena in Microtubes with Baffle Configuration. *Procedia Technology*. 22: 243-250.
DOI: https://doi.org/10.1016/j.protcy.2016.01.075.

[15] Wibowo, D., Zhao, C., and He, Y. 2019. *Chapter 2 Fluid Properties and Hydrodynamics of Microfluidic Systems*. Microfluidics for Pharmaceutical Applications. Elsevier: Amsterdam, The Netherlands. 37-77
DOI: https://doi.org/10.1016/B978-0-12-812659-2.00002-8.

[16] Juraeva, M., & Kang, D. J. 2020. Mixing Performance of a Cross-Channel Split-and-Recombine Micro-Mixer Combined with Mixing Cell. *Micromachines*. 11(7): 685.
DOI: https://doi.org/10.3390/mi11070685.

[17] Bayareh, M., Ashani, M. N., and Usefian, A. 2020. Active and Passive Micromixers: A Comprehensive Review. *Chemical Engineering and Processing-Process Intensification*. 147: 107771.
DOI: https://doi.org/10.1016/j.cep.2019.107771.

[18] Pawinanto, R. E., Yunas, J. and Hashim, A. M. 2020. Micropillar Based Active Microfluidic Mixer for the Detection of Glucose Concentration. *Microelectronic Engineering*. 234: 111452.
DOI: https://doi.org/10.1016/j.mee.2020.111452.

[19] Hasanah, L., Nurvadila, D. F., Pawinanto, R. E., Mulyanti, B., Wulandari, C., Aminudin, A., & Yunas, J. 2022. A Passive Micromixer with Koch Snowflakes Fractal Obstacle in Microchannel. *Journal of Applied Fluid Mechanics*. 15(5): 1333-1344.
DOI: http://dx.doi.org/10.47176/jafm.15.05.1015.

[20] Suh, Y. K. and Kang, S. 2010. A Review on Mixing in Microfluidics. *Micromachines*. 1(3): 82-111.
DOI: https://doi.org/10.3390/mi1030082.

[21] Rohman A. S, Mulyanti B, Pawinanto R. E., and Pantjawati A. B. The Optimization of Microfluidic Mixer Based on Meander Structure. *3rd International Conference of Computer and Informatics Engineering IC2IE*. 80-84.
DOI: http://dx.doi.org/10.1109/IC2IE50715.2020.9274668.

[22] Fang, W. F. and Yang, J. T. 2009. A Novel Microreactor with 3d Rotating Flow to Boost Fluid Reaction and Mixing of Viscous Fluids. *Sensors and Actuators B: Chemical*. 140(2): 629-642.
DOI: https://doi.org/10.1016/j.snb.2009.05.007.

[23] Chung, C. K., and Shih, T. R. 2007. A Rhombic Micromixer with Asymmetrical Flow for Enhancing Mixing. *Journal of Micromechanics and Microengineering*. 17(12): 2495.
DOI: https://doi.org/10.1088/0960-1317/17/12/016.

[24] Schönfeld, F., Hessel, V. and Hofmann, C. 2004. An Optimised Split-and-Recombine Micro-Mixer with Uniform Chaotic Mixing. *Lab on a Chip*. 4(1): 65-69.
DOI: http://dx.doi.org/10.1039/b310802c.